

## Coencapsulation of *trans*-Dehydrocrotonin and *trans*-Dehydrocrotonin:hydroxypropyl- $\beta$ -cyclodextrin into Microparticles

Waldenice A. Morais,<sup>a,b</sup> Benício de Barros Neto,<sup>c,†</sup> Isabella M. F. Cavalcanti,<sup>a</sup>  
Francisco H. Xavier Junior,<sup>a</sup> Nereide S. Santos-Magalhães<sup>a</sup> and Maria Aparecida M. Maciel<sup>\*,d</sup>

<sup>a</sup>Laboratório de Imunopatologia Keizo-Asami (LIKA), Universidade Federal de Pernambuco (UFPE),  
Av. Prof. Moraes Rego, 1235, Cidade Universitária, 50670-901 Recife-PE, Brazil

<sup>b</sup>Departamento de Farmácia, Universidade Federal do Rio Grande do Norte (UFRN),  
Campus Universitário, s/n, Lagoa Nova, 59012-570 Natal-RN, Brazil

<sup>c</sup>Departamento de Ciências Exatas e da Natureza, Universidade Federal de Pernambuco (UFPE),  
Av. Prof. Luís Freire, s/n, Cidade Universitária, 50740-540 Recife-PE, Brazil

<sup>d</sup>Departamento de Química, Universidade Federal do Rio Grande do Norte (UFRN),  
Campus Universitário, s/n, Lagoa Nova, 59078-970 Natal-RN, Brazil

The aim of this study was to develop and characterize poly- $\epsilon$ -caprolactone (PCL) and poly(D,L-lactic-co-glycolic)-acid (PLGA) microparticles containing coencapsulated *trans*-dehydrocrotonin (*t*-DCTN) and *t*-DCTN:hydroxypropyl- $\beta$ -cyclodextrin inclusion complex (*t*-DCTN:HP- $\beta$ -CD), with *t*-DCTN loaded at concentrations ranging from 11.25 to 45.00 mg. A preformulation study was carried out using a 2<sup>4+1</sup> fractional factorial design. Microparticles were prepared using the double w/o/w emulsion-solvent evaporation method. The coencapsulated *t*-DCTN:HP- $\beta$ -CD-loaded PLGA microparticles (*t*-DCTN/*t*-DCTN:HP- $\beta$ -CD/PLGA-MPs) presented a smaller particle size ( $9.6 \pm 0.1 \mu\text{m}$ ) and higher drug loading ( $13.93 \pm 0.05\%$ , corresponding to  $90.1 \pm 0.3\%$  of encapsulation efficiency, EE) and *t*-DCTN-loaded PLGA microparticles (*t*-DCTN/PLGA-MPs) presented particle size of  $37.0 \pm 0.2 \mu\text{m}$  and drug loading of  $10.12 \pm 0.01\%$  (EE of  $71.2 \pm 0.1\%$ ). The coencapsulation of *t*-DCTN and *t*-DCTN:HP- $\beta$ -CD into PLGA microparticles increased drug loading (50%) and improved the drug controlled release ( $k_2 = 0.0475$  and  $D_c = 0.0475 \times 10^{-11} \text{ cm}^2 \text{ s}^{-1}$ ). Taking into account these findings, new oral formulation of PLGA microparticles containing coencapsulated *t*-DCTN and *t*-DCTN:HP- $\beta$ -CD are available as biocompatible drug delivery systems for further pharmacological purposes.

**Keywords:** *trans*-dehydrocrotonin, cyclodextrin, PLGA microparticles, coencapsulation, fractional factorial design

## Introduction

The diterpene 19-*nor*-clerodane *trans*-dehydrocrotonin (*t*-DCTN) is the major compound isolated from the stem bark of *Croton cajucara* Benth (Euphorbiaceae).<sup>1</sup> Earlier studies showed *t*-DCTN as an important bioactive compound that presents numerous biological activities, among them anti-ulcerogenic,<sup>2</sup> anti-tumorigenic<sup>3</sup> and anti-glycemic.<sup>4</sup> However, the therapeutic applications of this natural product are hindered by the *t*-DCTN-dose-

dependent cytotoxicity in hepatocytes<sup>5</sup> and also its low solubility in water.<sup>1</sup> These problems could be solved by the encapsulation of *t*-DCTN into polymeric delivery systems that modulate its therapeutic dose, bioavailability and toxic effects.

Polymeric microparticles have usually been employed as attractive drug delivery systems to compensate the low oral bioavailability of certain drugs. Polymeric microparticles are able to provide controlled drug delivery in the therapeutic range, allowing a less frequent administration and reducing toxic effects, thereby increasing patient compliance with treatment. Biocompatible and biodegradable polymers with a safety profile for human use, such as poly- $\epsilon$ -caprolactone

\*e-mail: mammaciell@quimica.ufrn.br

†In memoriam

(PCL) and poly(D,L-lactic-*co*-glycolic)-acid (PLGA), are the most widely used materials in the preparation of drug delivery systems. Several methods have been described to prepare microparticles, including double emulsion-solvent evaporation.<sup>6-10</sup>

Microparticle characteristics such as particle size, drug encapsulation efficiency and drug release properties can be affected by the concentration and viscosity of solvent, cosolvent, stabilization, surfactant, drug and polymer types. These variables effects can be quantitatively assessed by means of factorial experimental design, which is usually the starting point for the optimization of pharmaceutical formulations.<sup>11</sup>

Inclusion complexes of drugs with cyclodextrins (CDs) have been entrapped into microparticles in order to optimize the properties of solubility, stability, release and therapeutic of the biocompounds.<sup>12,13</sup> Based on a novel approach aiming at controlled profile for release of hypnotic agent zolpidem (ZP) with simultaneous use of hydroxypropyl- $\beta$ -cyclodextrin (HP- $\beta$ -CD) added to the aqueous phase and ZP to the organic phase on PLGA and poly(DL-lactide) (PDLLA) microparticles, it was possible to evaluate the coencapsulated effect of free drug ZP and HP- $\beta$ -CD.<sup>14</sup> Generally the coencapsulation strategy refers to simultaneous encapsulation of different molecules such as drugs, markers, chemical entities, polymers.<sup>14,15</sup>

HP- $\beta$ -CD is a cyclodextrin (CD) with a large hydrophobic cavity (0.70 nm) and is well tolerated in human beings, which turns it suitable for *in vivo* applications. HP- $\beta$ -CD is the preferable cyclodextrin derivative on the pharmaceutical industry to be used for improving drug solubility or drug complexation, mainly because of its highly water-solubility and low toxicity, and the capability to form more stable drug-inclusion complexes.<sup>16-18</sup>

In this sense, *trans*-dehydrocrotonin was earlier complexed with  $\beta$ -cyclodextrin and the *t*-DCTN-inclusion complex showed to be able to reduce *t*-DCTN cytotoxicity in both rat hepatocytes (3.5-fold; IC<sub>50</sub> = 500 and 144  $\mu$ M) and V79 fibroblasts (1.7-fold; IC<sub>50</sub> = 676 and 400  $\mu$ M) for free and complexed drug, respectively.<sup>19</sup>

In the sequence, it was developed a new formulation such as *t*-DCTN-loaded PLGA microparticles and for that it was achieved high drug encapsulation efficiency (85.5  $\pm$  3.9%).<sup>20</sup> This system presents an initial release of 19.4% at 2 h and attained 55.6% maximum drug release within twenty-five hours. The hypoglycemic effect of the *t*-DCTN-loaded PLGA microparticles showed 26.8% reduction in glucose levels in animals, compared with 14.3% reduction by treatment using free *t*-DCTN.

The aims of the present study were to optimize *t*-DCTN loading in biodegradable PCL and PLGA

microparticles using a two-level factorial experimental design, and to improve drug loading by using the concept of drug coencapsulation with drug:cyclodextrin inclusion complexes (*t*-DCTN and *t*-DCTN:HP- $\beta$ -CD). The physicochemical and release characteristics of *t*-DCTN-loaded microparticles were investigated for further pharmacological purposes.

## Experimental

### Materials

Plant material was collected in Jacundá, Pará State (Amazon region, Brazil) and identified by Nelson A. Rosa. A voucher specimen (No. 247) has been stored in the Herbarium of the Museu Paraense Emílio Goeldi (Belém-PA, Brazil). The diterpene 19-*nor*-clerodane *trans*-dehydrocrotonin (*t*-DCTN) was extracted and purified from the stem bark of *Croton cajucara* Benth, as previously described.<sup>1</sup> Poly(D,L-lactic-*co*-glycolic)-acid (PLGA 50/50, inherent viscosity 0.57 dL g<sup>-1</sup>) was purchased from Birmingham Polymers (Alabama, USA). Poly- $\epsilon$ -caprolactone (PCL, MW ca. 14,000 Da), polyvinyl alcohol (PVA, MW ca. 13,000-17,000 Da), polyethylene glycol (PEG, MW ca. 4,000 Da), trehalose and 2-hydroxypropyl- $\beta$ -cyclodextrin (HP- $\beta$ -CD, MW ca. 1,380, degree of substitution ca. 0.6) were acquired from Sigma-Aldrich (St. Louis, USA). Tween 80<sup>®</sup> was supplied by Labsynth (São Paulo, Brazil). Purified water was produced by a water purification system (UP 900, Human Corporation, Korea). All reagents used were of analytical grade.

### Preparation of *t*-DCTN:HP- $\beta$ -CD inclusion complex

The *t*-DCTN:HP- $\beta$ -CD inclusion complex (1:1 molar ratio) was prepared using the freeze-drying technique. Appropriate amounts of drug and HP- $\beta$ -CD were dissolved in ethanol:water solution (1:1), stirred for 48 h at 25 °C, cooled by immersion in liquid nitrogen and lyophilized (EZ-DRY, FTS System, US) for 48 h. The amount of *t*-DCTN in the inclusion complex was determined using a UV-Vis-validated method.<sup>17</sup> The standard curve of *t*-DCTN in acetonitrile was prepared at concentrations ranging from 1 to 20  $\mu$ g mL<sup>-1</sup>. To extract the drug from the inclusion complex, a sample of *t*-DCTN:HP- $\beta$ -CD, equivalent to 1 mg of *t*-DCTN, was weighed and mixed with 10 mL of methanol and acetonitrile mixture (1:10). The sample was then diluted with acetonitrile in order to produce a theoretical drug concentration of 10  $\mu$ g mL<sup>-1</sup>. This procedure was performed in triplicate.

## Preparation of microparticles

Two different polymeric matrices of PCL and PLGA were tested to encapsulate *t*-DCTN into microparticles resulting in the following formulations: (1) *t*-DCTN/PCL-MPs; (2) *t*-DCTN:HP- $\beta$ -CD/PCL-MPs; (3) *t*-DCTN/PLGA-MPs; (4) *t*-DCTN:HP- $\beta$ -CD/PLGA-MPs and the (5) coencapsulated *t*-DCTN/*t*-DCTN:HP- $\beta$ -CD/PLGA-MPs. Initially, preformulation studies of unloaded PCL microparticles were conducted using a  $2^{4+1}$  fractional factorial design in order to optimize the system. Next, PLGA microparticles were produced in the same conditions as PCL microparticles in order to evaluate the influence of the polymer matrix on drug encapsulation into microparticles. The real factor levels were coded as shown in Table 1. The effects of four independent factors of the simple (*i*) and multiple (*ii*) emulsions were evaluated as follows: (*i*) factor 1 (PEG<sub>A1</sub> = 50, 125 or 200 mg) and factor 2 (inner aqueous phase volume, V<sub>A1</sub> = 1, 2 or 3 mL); (*ii*) factor 3 (PVA<sub>A2</sub> = 0.5, 1.25 or 2%) and factor 4 (aqueous continuous phase volume, V<sub>A2</sub> = 30, 65 or 100 mL). The optimum response variables for microparticles were a volume mean diameter ( $d_v$ ) less than 10  $\mu$ m and a particle size distribution (span) below 2. A design matrix was then generated with a randomized order and consisted of eleven batches of microparticles (from M1 to M11). To provide an estimate of the pure error of the responses, a central point run in triplicate was provided (M9-M11). The statistical analyses of the data were carried out using the Statistica® software (version 6).

**Table 1.** Factor levels and response variables used in the  $2^{4+1}$  fractional factorial design to prepare unloaded microparticles

Factors	Coding		
	-1	0	+1
Simple emulsion			
(1) PEG (PEG <sub>A1</sub> ) / mg	50	125	200
(2) Aqueous phase volume (V <sub>A1</sub> ) / mL	1	2	3
Multiple emulsion			
(3) PVA (PVA <sub>A2</sub> ) / %	0.5	1.25	2
(4) Aqueous phase volume (V <sub>A2</sub> ) / mL	30	65	100
Response variables	volume mean diameter ( $d_v$ ) particle size distribution (span)		

PEG: Polyethylene glycol; PVA: polyvinyl alcohol.

The microparticles were prepared using a water-in-oil-in-water (w/o/w) double emulsion followed by the solvent evaporation technique. Initially, a simple emulsion (w/o) was prepared by dissolving PCL (225 mg) in dichloromethane (6 mL). The organic solution was emulsified with 1-3 mL phosphate buffer solution (pH 7.4) containing PEG (50-200 mg) using an ultra-turrax T25 (IKA, Germany) at

8,000 rpm for 1 min. This first emulsion was then added in the outer aqueous phase (30-100 mL) containing PVA (0.5-2%, m/v) and emulsified at 8,000 rpm for 30 s, resulting in a double emulsion (w/o/w). This emulsion was then maintained under agitation at 400 rpm for 2 h allowing the solvent evaporation. The microparticles were recovered by centrifugation (Kubota KN-70 centrifuge, Japan) at 3,000 rpm for 10 min and rinsed three times with distilled water to remove the excess emulsifiers. Finally, the microparticles were dispersed in 2 mL of trehalose aqueous solution (1%, m/v), frozen at -80 °C and lyophilized (EZ-DRY, FTS System, USA) at 200 mbar for 48 h. Lyophilized microparticles were stored at 25  $\pm$  1 °C in a vacuum desiccator.

Based on the factorial design results for the unloaded PCL microparticles, PCL and PLGA microparticles containing *t*-DCTN (11.25-22.50 mg) or *t*-DCTN:HP- $\beta$ -CD inclusion complex (11.25-22.50 mg) were prepared. *t*-DCTN was dissolved in the organic phase and *t*-DCTN:HP- $\beta$ -CD in the aqueous phase. In the case of coencapsulation, *t*-DCTN was dissolved in the organic phase and *t*-DCTN:HP- $\beta$ -CD in the aqueous phase of the simple emulsion.

## Characterization of microparticles

### Particle size analysis

The volume mean diameter and size distribution of the microparticles were determined using the laser diffraction technique (particle size analyzer, Microtrac® S3500, USA). Samples of lyophilized microparticles (10 mg) were dispersed in Tween 80® solution (0.04%, m/v), sonicated for 10 min and then analyzed. The span values were calculated using the equation 1.

$$\text{Span} = d_{(v,0.9)} - d_{(v,0.1)} / d_{(v,0.5)} \quad (1)$$

where  $d_{(v,0.9)}$ ,  $d_{(v,0.5)}$  and  $d_{(v,0.1)}$  are the volume mean diameters, expressed in  $\mu$ m, determined at the 90<sup>th</sup>, 50<sup>th</sup> and 10<sup>th</sup> particle distribution percentiles, respectively.

### Zeta potential measurements

The surface charge of the microparticles was evaluated by electrophoretic mobility ( $\mu$ E) measurements using a Zeta-Meter System 3.0<sup>+</sup> (Zeta-Meter, USA). Samples of microparticles (0.5%) were dispersed in 1 mM NaCl, sonicated for 10 min and analyzed at 25 °C. The results are reported as the mean of ten runs and expressed by the zeta potential ( $\zeta$ , mV).

### Morphological analyses

The microscopic aspect of microparticles was evaluated using scanning electron microscopy (SEM, FEI, Quanta

200 FEG, Hillsboro, USA). The samples were prepared from dispersion of lyophilized microparticles in deionized water. The dispersion of microparticles was dropped onto a piece of silica wafer and dried in a desiccator. Next, the wafer piece was sealed with colloidal gold on stubs for low vacuum analysis at 10 kV and magnification of approximately 5,000 $\times$ .

#### Porosity analysis

The porosity parameters of the microparticles were evaluated using the gas adsorption technique. Measurements were performed using the accelerated surface area and porosimetry system (ASAP 2420, Micrometrics, Norcross, USA). Before analysis, a sample of lyophilized microparticles (100 mg) was placed in a volumetric tube, degassed under vacuum at 20 °C for 48 h, immersed in liquid nitrogen and then exposed to nitrogen under controlled pressure. The pressure at which adsorption equilibrium occurred was measured and the ideal gas equation applied to determine the amount of gas adsorbed on the surface of the microparticles. Silica-alumina pellets (specific surface area 215  $\pm$  6 m<sup>2</sup> g<sup>-1</sup>; mean pore diameter of 11.5 nm) were used as standard. The specific surface area was calculated using the Brunauer-Emmett-Teller (BET) method.<sup>21</sup> The pore size distribution was determined by the adsorption branch of the N<sub>2</sub> isotherm (1.7-300 nm diameters range) using the Barret-Joyner-Halenda (BJH) model.<sup>7</sup>

#### Drug encapsulation efficiency and drug loading

Lyophilized microparticles (5 mg) were dissolved in a mixture of dichloromethane and methanol (25 mL, 3:2, v/v) and sonicated for 10 min. The amount of *t*-DCTN in the microparticles was determined at 238 nm using a standard curve of *t*-DCTN in methanol, at concentration ranging from 1 to 20  $\mu$ g mL<sup>-1</sup>. The drug content values were used to calculate the drug loading (equation 2) and encapsulation efficiency (equation 3). The experiments were carried out in triplicate.

$$DL = \frac{t\text{-DCTN}_{\text{content}}}{t\text{-DCTN}_{\text{microparticle weight}}} \times 100 \quad (2)$$

$$EE = \frac{t\text{-DCTN}_{\text{content}}}{t\text{-DCTN}_{\text{total}}} \times 100 \quad (3)$$

where DL is drug loading, EE is drug encapsulation efficiency and *t*-DCTN is the biocompound *trans*-dehydrocrotonin. The content is the measured drug concentration and total means the theoretical amount of drug in microparticles.

#### *In vitro* drug release kinetics

The release kinetics of *t*-DCTN into microparticles was carried out using the dissolution technique in *sink* conditions, considering *t*-DCTN solubility at pH 7.4 PBS (37 °C) equal to 36.6  $\pm$  3.2  $\mu$ g mL<sup>-1</sup>.<sup>19</sup> Samples of microparticles were placed in 200 mL of phosphate buffer (0.2 M, pH 7.4) at 37  $\pm$  1 °C under magnetic stirring. At predetermined time intervals an aliquot of the release medium (1 mL) was withdrawn and replaced by fresh medium. After filtration of samples (0.22  $\mu$ m membrane filter, Millipore®, USA), the *t*-DCTN content was determined using a spectrophotometer at 244 nm.<sup>22</sup>

The *in vitro* release profiles of *t*-DCTN from different microparticle formulations were plotted as the percentage of released *t*-DCTN as a function of time. The kinetic experiments were conducted in triplicate.

The experimental release data were fitted using an exponential simplified model derived from the analytical solution for the Fick's second law for spherical microparticles.<sup>23</sup>

$$\frac{M_t}{M_\infty} = 1 - \frac{6}{\pi^2} \sum_{n=1}^{\infty} \exp\left(-\frac{n^2\pi^2}{R^2}Dt\right) \quad (4)$$

A first order approximation of the equation 4 establishes that:

$$\frac{M_t}{M_\infty} \cong 1 - \frac{6}{\pi^2} \exp\left(-\frac{\pi^2}{R^2}Dt\right) \quad (5)$$

where D is the diffusion coefficient and R is the average radius of the microparticles.

The approximated model used to fit experimental data is represented as follows:

$$M_t / M_\infty = (1 - k_1 e^{-k_2 t}) \quad (6)$$

where M<sub>t</sub> and M<sub>∞</sub> are the absolute cumulative amount of drug released at time t and infinite time, respectively; k<sub>1</sub> is a model constant and k<sub>2</sub> is a rate constant associated with the drug diffusion coefficient in the polymeric matrix.<sup>23</sup>

#### Statistical analysis

All data were statistically analyzed and expressed as mean  $\pm$  standard deviation (SD). The means of two groups were compared using the non-paired Student's *t*-test. When comparing multiple groups, one-way analysis of variance (ANOVA) was applied using the Tukey multiple comparison procedure. The analyses were performed using the Graph Pad Prism (version 5.0, La Jolla, CA, USA). The statistical data were considered significant at *p* < 0.05.

**Table 2.** Volume mean diameter ( $d_v$ ) and particle size distribution (span) of unloaded PCL microparticles obtained by the emulsion/solvent evaporation technique using a  $2^{4-1}$  fractional factorial design<sup>a</sup>

Microparticle	Factor				Response variables	
	1 (PEG <sub>A1</sub> )	2 (V <sub>A1</sub> )	3 (PVA <sub>A2</sub> )	4 (V <sub>A2</sub> )	$d_v \pm SD / \mu\text{m}$	Span
M1	+1	-1	-1	+1	28.4 $\pm$ 0.3	2.02
M2	-1	-1	+1	+1	26.0 $\pm$ 0.5	1.29
M3	+1	+1	+1	+1	14.1 $\pm$ 1.1	1.62
M4	-1	+1	-1	+1	8.1 $\pm$ 0.1	2.51
M5	-1	+1	+1	-1	13.0 $\pm$ 0.6	4.76
M6	-1	-1	-1	-1	14.7 $\pm$ 0.9	1.79
M7	+1	-1	+1	-1	7.8 $\pm$ 0.2	3.23
M8	+1	+1	-1	-1	6.7 $\pm$ 0.4	3.61
M9	0	0	0	0	20.8 $\pm$ 1.8	1.56
M10	0	0	0	0	18.6 $\pm$ 0.4	1.35
M11	0	0	0	0	22.9 $\pm$ 1.5	1.76

PCL = 225 mg. PEG: Polyethylene glycol; PVA: polyvinyl alcohol; PCL: poly- $\epsilon$ -caprolactone; SD: standard deviation. <sup>a</sup>Levels are coded as indicated in Table 1.

## Results and Discussion

### Preformulation study of PCL microparticles

The factorial design was used to select the ideal formulation of PCL microparticles for further incorporation of *t*-DCTN and *t*-DCTN:HP- $\beta$ -CD inclusion complex. A  $2^{4-1}$  fractional factorial design was carried out to evaluate the effect of variables on the size pattern of empty PCL microparticles obtained using the double emulsion/solvent evaporation technique.

The factors of the simple emulsion (PEG<sub>A1</sub> and V<sub>A1</sub>) and the double emulsion (PVA<sub>A2</sub> and V<sub>A2</sub>) strongly influenced the response variables  $d_v$  and span of the microparticles as shown in Table 2. The values of volume mean diameter of empty PCL microparticles ranged from 6.68 to 28.41  $\mu\text{m}$  and span values from 1.56 to 4.76.

The interaction effects of factors in the factorial design of empty PCL microparticles are summarized in Table 3. The effect value indicates the magnitude of the impact of each factor as well as its interactions. The signal effect, positive (+) or negative (-), indicates when the response variable is modified as a function of the variation factor. A positive effect means that the output increases with an increase in the variable level and a negative effect means that the output increases with a decrease in the variable level.<sup>10</sup> The data clearly indicate the significant effects of the factors V<sub>A1</sub> and V<sub>A2</sub> on  $d_v$  and span of PCL microparticles ( $R^2 = 0.989$ ). The internal aqueous phase volume had a negative effect (-8.20) and the external aqueous phase

volume a positive effect (8.61) on particle size. This means that a decrease in the  $d_v$  can be achieved with an increase in V<sub>A1</sub> and a decrease in V<sub>A2</sub>. V<sub>A1</sub> and V<sub>A2</sub> present main positive (0.835) and negative (-1.488) effects in the span, respectively. Thus a change in one of the significant factors of the factorial design (V<sub>A1</sub> and V<sub>A2</sub>) causes opposite effects on the size and span of the PCL microparticles. Taking into account the formulation M8 (V<sub>A1</sub> = 3 mL and V<sub>A2</sub> = 30 mL), a smaller  $d_v$  (6.68  $\pm$  0.43  $\mu\text{m}$ ) and a higher span (3.61) were found.

**Table 3.** The interaction effects estimated from the response values in the  $2^{4-1}$  fractional factorial design of unloaded PCL microparticles

Factor	Effect 1 ( $d_v$ )	Effect 2 (span)
1	-1.21	0.033
2	<b>-8.20</b>	<b>0.853</b>
3	0.19	0.432
4	<b>8.61</b>	<b>-1.488</b>
1 by 2	1.61	<b>-1.243</b>
1 by 3	<b>-7.92</b>	-0.443
1 by 4	5.39	-0.113

PCL: poly- $\epsilon$ -caprolactone;  $d_v$ : volume mean diameter. The values showed in bold represent the factors that present statistical significance ( $p < 0.05$ ).

The significant interaction effects were 1 by 3 on  $d_v$  (-7.92), and 1 by 2 on span (-1.243) of the PCL microparticles. The results showed that the interaction of the factors PEG<sub>A1</sub> and PVA<sub>A2</sub> causes a decrease in  $d_v$



(7.82  $\mu\text{m}$ , M7), and the interaction of the factors  $\text{PEG}_{A1}$  and  $V_{A1}$  produced a decrease in the span of PCL microparticles. The fractional factorial design allowed the production of PCL microparticles with a smaller size ( $< 19 \mu\text{m}$ ) but higher span values ( $> 1.76$ , except for M2 and M3) in relation to M9, because of the counter acting effects of the factors on the response variables.

It has been reported that the particle size increases as the volume of the continuous phase ( $V_{A2}$ ) increases.<sup>24,25</sup> A large volume of the continuous phase provides a high concentration gradient of the organic solvent across the phase boundary by diluting the solvent, leading to a fast solidification of the polymer and increasing the size of the microparticles. For  $V_{A1}$ , an opposite effect was found, which increases when the inner aqueous phase increases the size of the microparticles. This effect is in disagreement with literature, but studies were carried out changing only one independent factor at time.<sup>24-26</sup> On the contrary, in the present study, interactions of four independent factors responsible to form microparticles were analyzed at the same time.

In the present study, the authors sought to produce microparticles with a mean particle size  $< 10 \mu\text{m}$  and a span value  $< 2$ . In this way a new microparticle formulation (M12) was produced based on statistical optimization: PCL (225 mg) and PEG (125 mg) with a  $V_{A1}$  of 2 mL to form the simple emulsion, and PVA (1.25%) and  $V_{A2}$  of 45 mL as the continuous phase. As expected, M12 presented a smaller  $d_v$  ( $6.45 \pm 0.53 \mu\text{m}$ ) and a slightly higher span (2.09) (Figure 1). The variation in the inner/external aqueous phase ( $w_1/w_2$ ) ratio had a great influence on the size of the PCL microparticles. The smallest value of  $d_v$  ( $6.45 \mu\text{m}$ ) was found for the  $w_1/w_2$  ratio of 1/22.5 (M12). However, small  $d_v$  values were also found for  $w_1/w_2$  ratios varying from 1/10 (6.7  $\mu\text{m}$ , M8) and 1/30 (7.8  $\mu\text{m}$ , M7).

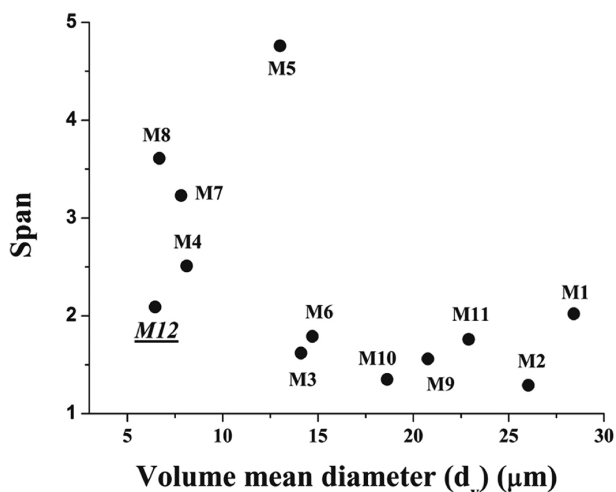


**Figure 1.** Scatterplot of volume mean diameter and span of unloaded PCL microparticles optimized using a  $2^{4-1}$  fractional factorial design.

The increase in particle size of PCL microparticles with an increase in the external aqueous phase volume can be attributed to a decrease in the mixing efficiency of emulsion phases associated with larger volumes during the stirring process. A reduction in mixing efficiency of emulsion phases probably produced an increase in the size of the simple emulsion droplets, resulting in the formation of large microparticles. The decrease in the diameter and the increase in the polydispersion (span) of microparticles with the increase in the internal aqueous phase volume were possibly caused by the increase in volume fraction of the dispersed continuous phase.<sup>7</sup> Using the w/o/w double emulsion technique, the viscosity of the polymer phase may also be influenced by the presence of the inner water phase. Thus, a decrease in viscosity in the dispersed phase of the microparticles resulted in a larger size distribution.<sup>20</sup>

PEG and PVA were used in order to stabilize the internal phase of the simple emulsion and the continuous phase of the multiple emulsion, respectively. As previously reported, the increase in surfactant concentrations causes a reduction in the size of microspheres.<sup>7,20</sup>

#### *t*-DCTN-loaded PCL and PLGA microparticles

The *t*-DCTN loading into PCL and PLGA microparticles ranged from 11.25 to 45.0 mg for a drug/polymer ratio ranging from 1:5 to 1:20 (Table 4). The presence of *t*-DCTN influenced the particle size of the PCL microparticles. A remarkable increase in the size and span of PCL microparticles has been observed with the augmentation in the initial amount of *t*-DCTN from 11.25 to 22.5 mg. The volume mean diameter of *t*-DCTN/PCL-MPs ranged from 25.8 to 49.3  $\mu\text{m}$  and the span from 1.39 to 2.12. It should be noted that the smallest size was found at the 1:20 drug/polymer ratio (25.8  $\mu\text{m}$ ). The presence of the drug can increase the viscosity of the dispersed phase, resulting in an increase in the size of droplets in the emulsification medium, which leads to an augmentation of the mean size of microparticles.<sup>7</sup>

The encapsulation efficiency of *t*-DCTN/PCL-MPs ranged from 18.1 (11.25 mg *t*-DCTN) to 49.7% (22.50 mg *t*-DCTN) and the drug loading increased from 0.79 to 4.06%. As expected, the *t*-DCTN loading in microparticles improved with the increase in the drug amount. In fact, it is well established that drug efficiency encapsulation into microparticles generally increases with an augmentation in the drug/polymer ratio.<sup>10</sup>

The volume mean size of *t*-DCTN/PLGA-MPs was smaller (16-37  $\mu\text{m}$ ) than *t*-DCTN/PCL-MPs (26-49  $\mu\text{m}$ ). The span values varied slightly from 0.81 to 1.42 for *t*-DCTN contents ranging from 11.25 to 45.00 mg (1:20-1:5

**Table 4.** Size properties, encapsulation efficiency and drug loading of *t*-DCTN in PCL and PLGA microparticles

Polymer	<i>t</i> -DCTN / mg	Drug:polymer ratio	Particle size ( $d_v \pm SD$ ) / $\mu\text{m}$	Span	DL $\pm$ SD / (% , m/m)	EE $\pm$ SD / %
PCL	11.25	1:20	25.8 $\pm$ 0.1	1.39	0.79 $\pm$ 0.01	18.1 $\pm$ 0.2
	15.00	1:15	42.2 $\pm$ 3.2	1.82	2.07 $\pm$ 0.02	34.2 $\pm$ 0.4
	22.50	1:10	49.3 $\pm$ 1.6	2.12	4.06 $\pm$ 0.02	49.7 $\pm$ 0.2
PLGA	11.25	1:20	15.8 $\pm$ 0.1	0.81	2.36 $\pm$ 0.02	58.8 $\pm$ 0.4
	15.00	1:15	16.3 $\pm$ 0.4	1.02	3.34 $\pm$ 0.01	62.7 $\pm$ 0.1
	22.50	1:10	14.6 $\pm$ 0.2	1.00	5.90 $\pm$ 0.03	75.7 $\pm$ 0.4
	45.00	1:5	37.1 $\pm$ 0.2	1.42	10.12 $\pm$ 0.01	71.2 $\pm$ 0.1

PCL: poly- $\epsilon$ -caprolactone (225 mg); PLGA: poly(D,L-lactic-*co*-glycolic)-acid (225 mg); EE: encapsulation efficiency; DL: drug loading;  $d_v$ : volume mean diameter; SD: standard deviation.

polymer/drug ratio). Drug encapsulation efficiency and drug loading increased from 58.8 to 75.7% and from 2.36 to 10.12% (m/m), respectively (Table 4). The increase in the drug/polymer ratio influenced the particle size of the PLGA microparticles due to the high affinity of *t*-DCTN with the PLGA matrix. This higher drug/polymer affinity causes an increased retention of the drug in the organic phase and improved emulsion stability during the formation of microparticles.<sup>27</sup>

#### *t*-DCTN:HP- $\beta$ -CD-and *t*-DCTN/*t*-DCTN:HP- $\beta$ -CD-loaded microparticles

Hydroxypropyl- $\beta$ -cyclodextrin (HP- $\beta$ -CD) was chosen to prepare inclusion complex because it was expected to

improve the aqueous solubility of *t*-DCTN in comparison to  $\beta$ -cyclodextrin ( $\beta$ -CD), as previously described.<sup>19</sup> Thus the incorporation of *t*-DCTN:HP- $\beta$ -CD inclusion complex (120 mg equivalent to 22.5 mg of *t*-DCTN) into PCL or PLGA microparticles (1:10 drug/polymer ratio) was carried out.

Figure 2 shows the physicochemical characteristics of PCL and PLGA microparticles containing *t*-DCTN and *t*-DCTN:HP- $\beta$ -CD inclusion complex. The encapsulation of *t*-DCTN or *t*-DCTN:HP- $\beta$ -CD into PCL matrix produced slight differences in the volume mean diameter and span (Figures 2a and 2b, respectively). Also, *t*-DCTN-loaded PCL microparticles presented  $d_v$  of 49.3  $\pm$  1.6  $\mu\text{m}$  and span of 2.12, while the *t*-DCTN:HP- $\beta$ -CD-loaded PCL microparticles presented  $d_v$  of 45.1  $\pm$  1.4  $\mu\text{m}$  and span of 1.95.

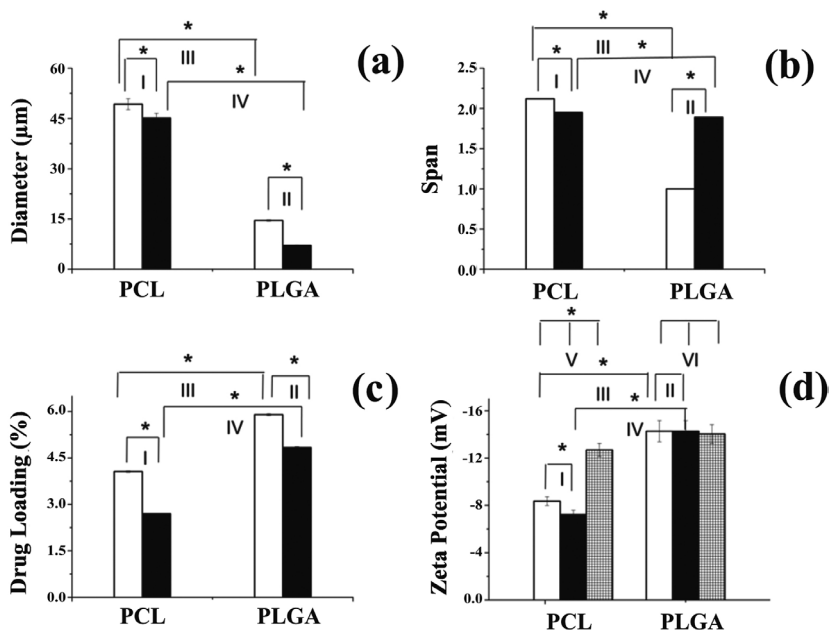


**Figure 2.** (a) Diameter; (b) span; (c) drug loading and (d) zeta potential of PCL and PLGA microparticles containing *t*-DCTN (white columns) or *t*-DCTN:HP- $\beta$ -CD inclusion complex (black columns), and unloaded microparticles (gray columns) at the 1:10 drug:polymer ratio. \*Statistically significant differences ( $p < 0.05$ ): (I) *t*-DCTN/PCL-MPs and *t*-DCTN:HP- $\beta$ -CD/PCL-MPs; (II) *t*-DCTN/PLGA-MPs and *t*-DCTN:HP- $\beta$ -CD/PLGA; (III) *t*-DCTN/PCL and *t*-DCTN/PLGA; (IV) *t*-DCTN:HP- $\beta$ -CD/PCL and *t*-DCTN:HP- $\beta$ -CD/PLGA; (V) *t*-DCTN/PCL, *t*-DCTN:HP- $\beta$ -CD/PCL and unloaded PCL; and (VI) *t*-DCTN/PLGA, *t*-DCTN:HP- $\beta$ -CD/PLGA and unloaded PLGA.

In the PLGA matrix, a significant decrease in particle size and an increase in span values were found in the presence of *t*-DCTN:HP- $\beta$ -CD ( $d_v = 7.1 \mu\text{m}$  and  $\text{span} = 1.89$ ) in comparison with *t*-DCTN ( $d_v = 14.6 \mu\text{m}$  and  $\text{span} = 1.00$ ) (Figures 2a and 2b, respectively).

Drug loading decreased from 4.1 to 2.7% and from 5.90 to 4.84% when *t*-DCTN:HP- $\beta$ -CD inclusion complex was incorporated into PCL and PLGA matrices, respectively (Figure 2c). This may be due in part to the fact that the droplets of the internal aqueous phase containing the soluble inclusion complex *t*-DCTN:HP- $\beta$ -CD can diffuse to the external aqueous phase more easily during the formation of microparticles.<sup>28</sup> PCL microparticles with a larger size presented a smaller drug loading than PLGA microparticles for both *t*-DCTN and *t*-DCTN:HP- $\beta$ -CD inclusion complex (Figure 2c). DL of the hydrophilic drug:inclusion complex encapsulated into PLGA microparticles is higher than into PCL-microparticles, considering that PLGA is less hydrophobic than PCL.<sup>29-31</sup> Based on these findings, the encapsulation of drugs into microparticles is affected by different factors such as particle size, drug/polymer interactions and emulsion stability during the preparation process of microspheres.

The zeta potential of PCL-based microparticles changed with the incorporation of *t*-DCTN ( $-8.4 \pm 0.4 \text{ mV}$ ) or *t*-DCTN:HP- $\beta$ -CD ( $-7.2 \pm 0.4 \text{ mV}$ ) in comparison with the empty microparticles ( $-12.7 \pm 0.6 \text{ mV}$ ) (Figure 2d). The slight decrease in zeta potential in relation to empty microparticles could be the result of a fraction of the drug being adsorbed on the particle surface, which may influence the surface charge. In contrast, no changes were observed after the incorporation of *t*-DCTN ( $-14.3 \pm 0.9 \text{ mV}$ ) or *t*-DCTN:HP- $\beta$ -CD ( $-13.9 \pm 0.9 \text{ mV}$ ) into PLGA microparticles ( $-14.0 \pm 0.8 \text{ mV}$ ), thus confirming the higher affinity of *t*-DCTN with the PLGA and its incorporation into the core of the polymeric matrix. As previously demonstrated, PLGA microparticles are negatively charged and this surface charge is associated with carboxylic groups of this polyester.<sup>27</sup>

The PLGA matrix provided higher drug loading, a smaller particle size and a narrow size distribution. This suggests a higher affinity between the drug and polymer matrix, thereby inducing higher drug incorporation into PLGA-based microparticles. Based on these findings, a study was performed to improve drug loading by changing the drug:polymer ratio from 1:10 to 1:5. Figure 2c shows that drug loading changed from  $5.90 \pm 0.03\%$  to  $10.12 \pm 0.01\%$  (m/m) for microparticles containing only *t*-DCTN (*t*-DCTN/PLGA-MPs).

Drug loading increased from  $4.84 \pm 0.02\%$  (m/m) for PLGA microparticles containing only *t*-DCTN:HP- $\beta$ -CD

at the 1:10 drug:polymer ratio, to  $13.93 \pm 0.05\%$  (m/m), containing *t*-DCTN and *t*-DCTN:HP- $\beta$ -CD coencapsulated at the 1:5 drug:polymer ratio. The particle size and span values changed from  $7.1 \pm 0.11 \mu\text{m}$  ( $\text{span} = 1.89$ ) for *t*-DCTN:HP- $\beta$ -CD to  $9.6 \pm 0.11 \mu\text{m}$  ( $\text{span} = 1.57$ ) for coencapsulated *t*-DCTN and *t*-DCTN:HP- $\beta$ -CD.

The presence of *t*-DCTN in the organic phase appears to have a great influence on the increased viscosity of the dispersed emulsion phase, as a higher particle size in microparticles containing only *t*-DCTN ( $37.1 \mu\text{m}$ ) was observed in comparison with *t*-DCTN and *t*-DCTN:HP- $\beta$ -CD coencapsulated at the 1:5 drug:polymer ratio ( $9.6 \mu\text{m}$ ). It has been reported that the increased viscosity in the dispersed phase may increase the size of microspheres.<sup>7</sup> The conception of drug coencapsulation with drug:cyclodextrin inclusion complex promoted in augmentation of drug loading into PLGA-microparticles by the fact of using both the free hydrophobic drug, placed in the organic phase during microparticles preparation, and *t*-DCTN:HP- $\beta$ -CD inclusion complex, which certainly improved the solubility of drug, placed in the aqueous phase during the preparation of the microparticles.

#### Morphological characteristics of microparticles

The morphological characteristics of the PCL and PLGA microparticles containing *t*-DCTN and *t*-DCTN:HP- $\beta$ -CD inclusion complex are shown in SEM micrographs (Figure 3). *t*-DCTN-loaded microparticles prepared with PCL were spherical in shape with a smooth surface (Figure 3a), while PLGA based-microparticles showed a porous surface and inner structure (Figure 3c). These results are in disagreement with the dense and nonporous microspheres obtained in our previous study. This can be attributed to the modification of the w/o/w parameters, such as the increase in the external aqueous phase and increased amount of PEG in the inner aqueous phase. All these parameters increased the osmotic gradient and resulting flux of water from  $w_2$  to  $w_1$ /polymer phase.<sup>20</sup>

The encapsulation of *t*-DCTN:HP- $\beta$ -CD inclusion complex into the PLGA microparticles caused a significant change in the morphology (Figures 3b and 3d), an effect unrelated to the polymer matrix. This indicates that the presence of the inclusion complex in the internal aqueous phase caused a change in the solvent evaporation rate, reducing the porosity effect found in the incorporation of the drug alone. PLGA microparticles containing *t*-DCTN and *t*-DCTN:HP- $\beta$ -CD coencapsulated at the 1:5 drug:polymer ratio exhibited morphological characteristics analogous to PLGA microparticles containing only *t*-DCTN:HP- $\beta$ -CD at the 1:10 drug:polymer ratio (Figure 3e).



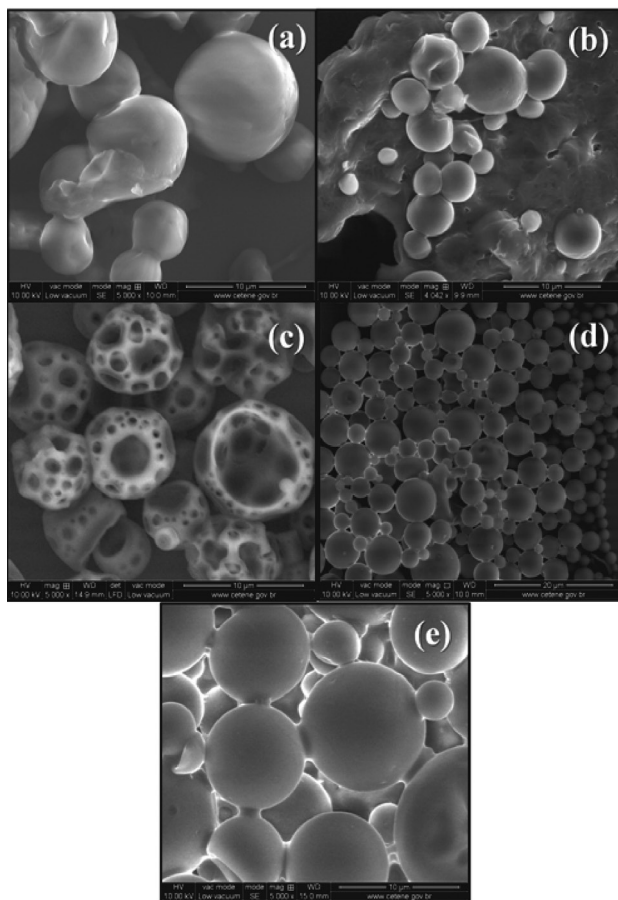


**Figure 3.** SEM micrographs of PCL and PLGA microparticles containing *t*-DCTN or *t*-DCTN:HP- $\beta$ -CD inclusion complex at the 1:10 drug:polymer ratio: (a) *t*-DCTN/PCL (5,000 $\times$ ); (b) *t*-DCTN:HP- $\beta$ -CD/PCL (4,042 $\times$ ); (c) *t*-DCTN/PLGA (5,000 $\times$ ); (d) *t*-DCTN:HP- $\beta$ -CD:PLGA (5,000 $\times$ ) and, (e) *t*-DCTN/*t*-DCTN:HP- $\beta$ -CD/PLGA coencapsulated at the 1:5 drug:polymer ratio (5,000 $\times$ ).

#### Porosity analysis of microparticles

The integrated area under the curve (AUC) applied to the incremental pore size distribution (PSD) of adsorption/desorption ( $AUC_{ads}/AUC_{des}$ ) branches of isotherm was determined in order to characterize the porosity of the microspheres. The results showed that the increase in the

specific surface area of microparticles ( $A_{BET}$ ) correlated with an increase in the porosity parameters (specific surface area and pore size distribution). This indicates that a higher specific surface area was associated with a higher porosity of the microparticles (Table 5). The PLGA microparticles containing only *t*-DCTN at the 1:10 drug:polymer ratio presented porosity parameter values ( $A_{BET} = 5.166 \text{ m}^2 \text{ g}^{-1}$ ;  $AUC_{ads} = 77.694$  and  $AUC_{des} = 34.799$ ) greater than PCL microparticles ( $A_{BET} = 2.874 \text{ m}^2 \text{ g}^{-1}$ ;  $AUC_{ads} = 61.539$  and  $AUC_{des} = 31.239$ ) (Table 5). However, the incorporation of *t*-DCTN:HP- $\beta$ -CD inclusion complex into microparticles produced a significant decrease in the porosity parameters, irrespective of the polymeric matrix, PCL ( $A_{BET} = 0.956 \text{ m}^2 \text{ g}^{-1}$ ;  $AUC_{ads} = 18.553$  and  $AUC_{des} = 5.063$ ) and PLGA ( $A_{BET} = 0.581 \text{ m}^2 \text{ g}^{-1}$ ;  $AUC_{ads} = 20.853$  and  $AUC_{des} = 5.405$ ).

The PLGA microspheres containing *t*-DCTN and *t*-DCTN:HP- $\beta$ -CD coencapsulated at the 1:5 drug:polymer ratio presented intermediate porosity parameter values ( $A_{BET} = 1.680 \text{ m}^2 \text{ g}^{-1}$ ;  $AUC_{ads} = 34.027$  and  $AUC_{des} = 11.784$ ) compared with the ones containing only *t*-DCTN. This emphasizes the greater influence of *t*-DCTN:HP- $\beta$ -CD inclusion complex on the porosity properties, as was also observed in the morphological analysis using SEM microscopy. The higher porosity of the PLGA microparticles containing only *t*-DCTN could be a result of the higher viscosity of the polymer solution and the smaller time required for PLGA reaction<sup>27</sup> as compared with PCL. It has already been reported that a more rapid flux of solvent across the o/w interface stresses the precipitated polymer film and may cause an increase in the porosity of the PLGA microparticles. Additionally, it suggests that the presence of PEG in the inner water phase could trigger strong interactions between PLGA/CH<sub>2</sub>Cl<sub>2</sub> systems. As previously demonstrated in the literature, a high osmotic pressure in the internal aqueous phase of the double emulsion generates an influx of water toward the inner aqueous phase. The occurrence of this process during particle hardening generally results in the formation of a

**Table 5.** Specific surface area and pore size distribution of the PCL and PLGA microparticles containing *t*-DCTN

Formulation	$A_{BET} / (\text{m}^2 \text{ g}^{-1})$	AUC incremental PSD / nm	
		Adsorption	Desorption
<i>t</i> -DCTN/PCL	2.874	61.539	31.239
<i>t</i> -DCTN:HP- $\beta$ -CD/PCL	0.956	18.553	5.063
<i>t</i> -DCTN/PLGA	5.166	77.694	34.799
<i>t</i> -DCTN:HP- $\beta$ -CD/PLGA	0.581	20.853	5.405
<i>t</i> -DCTN:HP- $\beta$ -CD: <i>t</i> -DCTN/PLGA <sup>a</sup>	1.680	34.027	11.784

PCL: poly- $\epsilon$ -caprolactone; PLGA: poly(D,L-lactic-*co*-glycolic)-acid;  $A_{BET}$ : specific surface area; PSD: pore size distributions. Drug:polymer ratio = 1:10.  
<sup>a</sup>1:5 drug/polymer ratio.

porous surface.<sup>32</sup> This porosity effect was less important in microspheres containing *t*-DCTN:HP- $\beta$ -CD because the presence of the inclusion complex might have inhibited the interaction of PEG with polymeric matrices.

The analysis of the N<sub>2</sub> adsorption isotherm profiles using the BJH model showed that the PCL and PLGA microspheres present meso- (2-50 nm) and macro-pores (> 50 nm) ranges according to the IUPAC classification (Figure 4). The BJH curves (incremental pore volume vs. pore size) showed a higher pore volume at the meso-pore range and a decrease in the population of mesopores smaller than 50 nm for microspheres containing *t*-DCTN:HP- $\beta$ -CD inclusion complex in both polymeric matrices. As previously reported for the specific surface area, the incorporation of *t*-DCTN:HP- $\beta$ -CD inclusion complex into microspheres decreased the pore volume. This decrease in pore volume of the microspheres can be ascribed to the change in the solvent removal rate and the longer reaction time required for *t*-DCTN:HP- $\beta$ -CD as compared to *t*-DCTN.

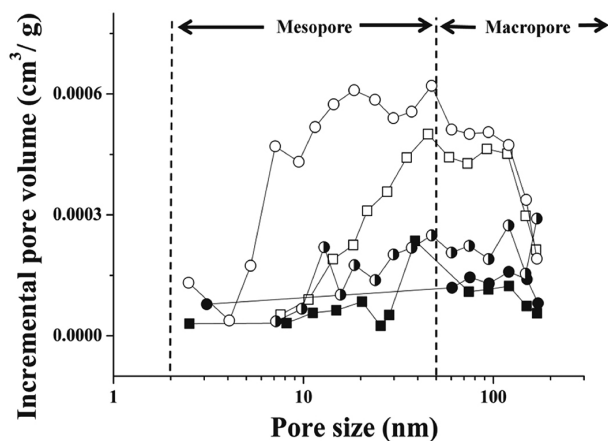


**Figure 4.** Pore size distribution (PZD) of microspheres determined using the BJH method applied to N<sub>2</sub> adsorption isotherms: (i) PCL microspheres: *t*-DCTN-loaded microparticles (white squares) and *t*-DCTN:HP- $\beta$ -CD-loaded microparticles at the 1:10 drug:polymer ratio (black squares); (ii) PLGA microspheres: *t*-DCTN-loaded microparticles (white circles) and *t*-DCTN:HP- $\beta$ -CD-loaded microparticles at the 1:10 drug:polymer ratio (black circles) and DCTN:HP- $\beta$ -CD/DCTN-loaded microparticles at the 1:5 drug:polymer ratio (white/black circles).

#### Release kinetics of *t*-DCTN and *t*-DCTN:HP- $\beta$ -CD inclusion complex from microparticles

In the present study, microparticles were prepared with two different polymeric matrix PCL and PLGA containing the drug (*t*-DCTN), the drug:cyclodextrin inclusion complex (*t*-DCTN:HP- $\beta$ -CD) or the coencapsulated drug and drug:inclusion complex (*t*-DCTN/*t*-DCTN:HP- $\beta$ -CD) and the *in vitro* drug release properties were evaluated. The release profiles of *t*-DCTN from microparticle formulations

are illustrated in Figures 5a and 5b: *t*-DCTN into PCL microparticles and *t*-DCTN into PLGA microparticles, respectively.

Analyzing kinetic data of *t*-DCTN from microparticles within the first 8 hours (Figure 5), a drug release of almost 78% from PCL-microparticles was verified, while only 40% was released from PLGA-microparticles within 2 hours of the kinetics. However, in the presence of HP- $\beta$ -CD in PLGA-microparticles, that is to say, the drug in cyclodextrin inclusion complex, a decrease of 45% on the drug release was found. In addition the coencapsulation of *t*-DCTN/*t*-DCTN:HP- $\beta$ -CD, reduced the drug release. This phenomenon can be explained by the porosity of microparticles. Moreover, the presence of HP- $\beta$ -CD diminished the porous and the mean volume diameter of PCL or PLGA microparticles containing *t*-DCTN.

The presence of the *t*-DCTN:HP- $\beta$ -CD inclusion complex improved physicochemical properties of microparticles by decreasing their porosity and the volume mean diameter. In fact, *t*-DCTN:HP- $\beta$ -CD improved drug loading and controlled drug release in PLGA-microparticles, probably due to the enhancement of the *t*-DCTN affinity by this matrix.

To understand the controlling drug diffusion mechanisms from these systems, experimental data of kinetics was fitted using a simplified exponential model (equation 6), based on the analytical solution of Fick's second law of diffusion<sup>23</sup> and fitted curves are presented in Figure 5. As it can see from Figure 5, a good agreement between theoretical and experimental data was found ( $r \geq 0.96$ ), indicating the simple mass transport diffusion mechanism of microparticulate systems.

The calculated kinetic parameters of *t*-DCTN-loaded microparticles using equation 6 are summarized in Table 6. The kinetic profile of *t*-DCTN into PLGA microparticles changed with a ten-fold decrease in the rate constant by the coencapsulation of *t*-DCTN:*t*-DCTN:HP- $\beta$ -CD ( $k_2 = 0.048$ ).

When performing the best-fit kinetic model using equation 6, the resulting values for the constant  $k_1$  should be of the order of magnitude of  $6/\pi^2 \cong 0.6079$ , with typical values in the range from 0 to 1. It is worthy to note that the variability of the experimental data and the terms eliminated in the original approach,<sup>23</sup> resulting in equation 6, also contribute to not result in the theoretical expected  $k_1$  value, which would be obtained only in an ideal scenario and considering the full model, taking into account the other despised terms of the equation. The  $k_1$  values obtained in fittings, which range between 0.2988 and 0.8724, are perfectly compatible, as expected when the validity of the kinetic model is assumed.

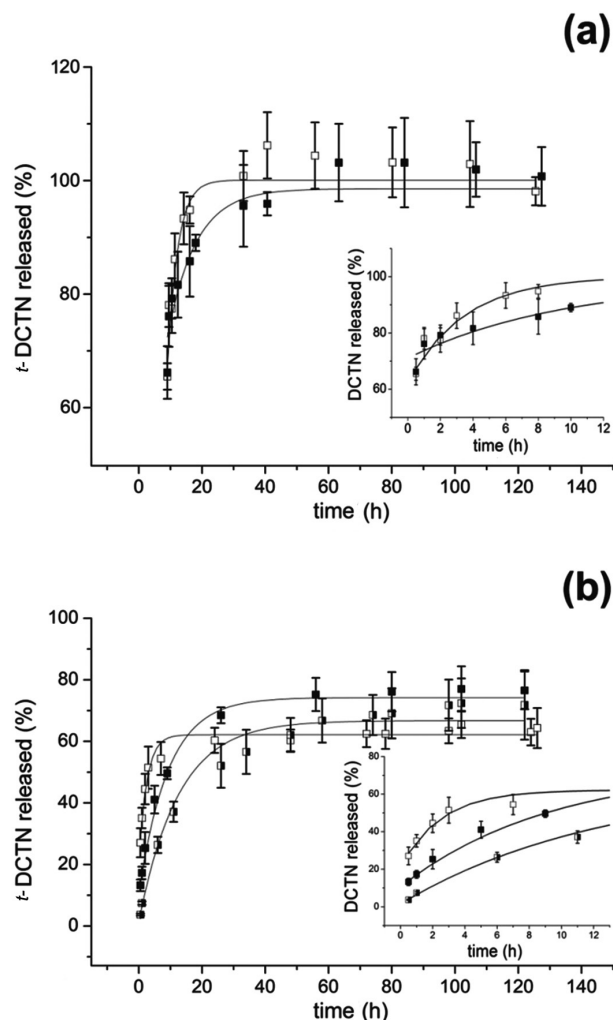


**Figure 5.** *In vitro* release of *t*-DCTN from microparticles: (a) PCL and (b) PLGA. *t*-DCTN-loaded microparticles (white squares); *t*-DCTN:HP- $\beta$ -CD-loaded microparticles (black squares) at the 1:10 drug:polymer ratio and *t*-DCTN:HP- $\beta$ -CD/*t*-DCTN-loaded microparticles at the 1:5 drug:polymer ratio (white/black squares). Each point represents the mean of three different experiments  $\pm$  SD. Lines represent the non-linear fitting of the Fickian diffusion model.

**Table 6.** Calculated release parameters and estimated diffusion coefficient of *t*-DCTN into PCL and PLGA microparticles containing *t*-DCTN, *t*-DCTN:HP- $\beta$ -CD inclusion complex and the coencapsulated *t*-DCTN/*t*-DCTN:HP- $\beta$ -CD, using an exponential model

<i>t</i> -DCTN Formulation (Drug:polymer ratio=1:10)	Exponential model $M_t / M_\infty = (1 - k_1 e^{-k_2 t})$		$r^2$	R / $\mu\text{m}$	$D_e \times 10^{11} /$ ( $\text{cm}^2 \text{ s}^{-1}$ )
	$k_1$	$k_2$			
<i>t</i> -DCTN/PCL	0.3155	0.2412	0.9623	24.65	4.1249
<i>t</i> -DCTN:HP- $\beta$ -CD/PCL	0.2988	0.1637	0.9818	22.65	2.3428
<i>t</i> -DCTN/PLGA	0.6993	0.4037	0.9860	7.30	6.0548
<i>t</i> -DCTN:HP- $\beta$ -CD/PLGA	0.7002	0.0626	0.9900	3.55	2.2204
<i>t</i> -DCTN:HP- $\beta$ -CD: <i>t</i> -DCTN/PLGA <sup>a</sup>	0.8724	0.0475	0.9911	4.80	3.0802

*t*-DCTN: *trans*-dehydrocrotonin; PCL: poly- $\epsilon$ -caprolactone; PLGA: poly(D,L-lactic-*co*-glycolic)-acid; HP- $\beta$ -CD: 2-hydroxypropyl- $\beta$ -cyclodextrin;  $r^2$ : correlation coefficient; R: mean radius of microparticles;  $D_e$ : effective diffusion coefficient; <sup>a</sup>drug:polymer ratio = 1:5.

Taking into account that  $k_2$  is the rate constant associated with the diffusion coefficient, to note that equation 6 results in a release rate decaying exponentially with time:

$$\frac{dM_t / M_\infty}{dt} \cong k_1 k_2 \cdot e^{-k_2 t} \quad (7)$$

Thus, the  $k_2$  value drives the rate decrease and very small values result in virtually constant rate over a long period of kinetics. For the last two results in Table 6, the  $k_2$  values decreased significantly about one order of magnitude. This features a slowest *t*-DCTN release compared with the *t*-DCTN:HP- $\beta$ -CD. The values of the  $k_2$  constant enable getting estimated effective diffusion coefficients ( $D_e$ ) of the *t*-DCTN in the microparticle formulations, according to:  $D_e = \frac{k_2 R^2}{\pi^2}$ . Thus the values of  $D_e$  were calculated and appended in Table 6.

The effective diffusion coefficient of *t*-DCTN was dependent on the type of polymeric matrix.  $D_e$  of *t*-DCTN in PCL is  $4.1249 \times 10^{-11} \text{ (cm}^2 \text{ s}^{-1}\text{)}$ , while a  $D_e$  of  $6.0548 \times 10^{-11} \text{ (cm}^2 \text{ s}^{-1}\text{)}$  was found for of *t*-DCTN in PLGA. In addition, the presence of *t*-DCTN:HP- $\beta$ -CD in the both PCL and PLGA matrices decreased the effective diffusion coefficient. It is worth to mention that *t*-DCTN:HP- $\beta$ -CD:*t*-DCTN/PLGA microparticles has smaller diameter of particles and as a result the lower diffusion coefficient, thereby resulting in a more controlled release of *t*-DCTN.

## Conclusions

The use of a factorial design represented a new approach to the study of the influence of formulation parameters on the size properties of empty PCL microspheres and optimization of these controlled drug delivery systems

to encapsulate *t*-DCTN and *t*-DCTN:HP- $\beta$ -CD inclusion complex using the double emulsion/solvent evaporation method. *t*-DCTN was successfully encapsulated into PCL and PLGA microspheres with a higher encapsulation efficiency and drug loading at the 1:10 drug/polymer ratio. The *t*-DCTN:HP- $\beta$ -CD inclusion complex decreased encapsulation efficiency, drug loading, particle size and porosity parameters at the 1:10 drug/polymer ratio in both polymeric matrices. The coencapsulation of *t*-DCTN with *t*-DCTN:HP- $\beta$ -CD inclusion complex at the 1:5 drug/polymer ratio increased encapsulation efficiency and drug loading in PLGA microspheres maintaining small values of particle size and span. The results suggest a smaller affinity of *t*-DCTN with the PCL matrix in relation to PLGA, owing to its lower encapsulation, higher modification of the surface charge, higher burst effect and faster release profiles regardless of particle size and porosity characteristics. From these findings novel oral formulations of PLGA microparticles containing *t*-DCTN and/or *t*-DCTN:HP- $\beta$ -CD were obtained for application in further *in vivo* pharmacological studies.

## Acknowledgments

W. A. M. is grateful for a PhD scholarship from the Brazilian Council for Scientific and Technological Development (CNPq). The authors thank the Pernambuco State Foundation for the Advancement of Science (FACEPE). This research was supported in part by the CNPq, Brazil (Grant No. 474071/2007-3).

## References

- Maciel, M. A.; Pinto, A. C.; Arruda, A. C.; Pamplona, S. G.; Vanderlinde, F. A.; Lapa, A. J.; Echevarria, A.; Grynberg, N. F.; Colus, I. M.; Farias, R. A.; Luna Costa, A. M.; Rao, V. S.; *J. Ethnopharmacol.* **2000**, *70*, 41.
- Rodriguez, J. A.; Hiruma-Lima, C. A.; Souza Brito, A. R.; *Hum. Exp. Toxicol.* **2004**, *23*, 455.
- Grynberg, N. F.; Echevarria, A.; Lima, J. E.; Pamplona, S. S.; Pinto, A. C.; Maciel, M. A.; *Planta Med.* **1999**, *65*, 687.
- Farias, R. A.; Rao, V. S.; Viana, G. S.; Silveira, E. R.; Maciel, M. A.; Pinto, A. C.; *Planta Med.* **1997**, *63*, 558.
- Rodriguez, J. A.; Haun, M.; *Planta Med.* **1999**, *65*, 522.
- Zidan, A. S.; Sammour, O. A.; Hammad, M. A.; Megrab, N. A.; Hussain, M. D.; Khan, M. A.; Habi, M. J.; *AAPS PharmSciTech* **2006**, *7*, E1.
- Li, M.; Rouaud, O.; Poncelet, D.; *Int. J. Pharm.* **2008**, *363*, 26.
- Vilos, C.; Velasquez, L. A.; *J. Biomed. Biotechnol.* **2012**, *2012*, 1.
- Dorati, R.; Genta, I.; Colzani, B.; Modena, T.; Bruni, G.; Tripodo, G.; Conti, B.; *AAPS PharmSciTech* **2015**, *16*, 1129.
- Soudry-Kochavi, L.; Naraykin, N.; Nassar, T.; Benita, S.; *J. Controlled Release* **2015**, *217*, 202.
- Bruns, R. E.; Scarminio, I. S.; Barros-Neto, B.; *Statistical Design - Chemometrics*, 1<sup>st</sup> ed.; Elsevier: Amsterdam, 2005.
- Sajeesh, S.; Sharma, C. P.; *Int. J. Pharm.* **2006**, *325*, 147.
- Filipović-Grčić, J.; Voinovich, D.; Moneghini, M.; Bećirević-Laćan, M.; Magarotto, L.; Jalšenjak, I.; *Eur. J. Pharm. Sci.* **2000**, *9*, 373.
- Trapani, G.; Lopodota, A.; Boghetich, G.; Latrofa, A.; Franco, M.; Sanna, E.; Liso, G.; *Int. J. Pharm.* **2003**, *268*, 47.
- Agashe, H.; Lagisetty, P.; Saho, K.; Bourne, D.; Grady, B.; Awasthi, V.; *J. Nano Res.* **2011**, *13*, 2609.
- Gould, S.; Scott, R. C.; *Food Chem. Toxicol.* **2005**, *43*, 1451.
- Loftsson, T.; Duchêne, D.; *Int. J. Pharm.* **2007**, *329*, 1.
- Gidwani, B.; Vyas, A.; *BioMed Res. Int.* **2015**, *2015*, 1.
- Correa, D. H.; Melo, P. S.; Carvalho, C. A.; Azevedo, M. B.; Duran, N.; Haun, M.; *Eur. J. Pharmacol.* **2005**, *510*, 17.
- Morais, W. A.; Costa, M. P.; Paixão, A. D.; Maciel, M. A.; Santos-Magalhães, N. S.; *J. Microencapsulation* **2009**, *26*, 529.
- Wischke, C.; Schwendeman, S. P.; *Int. J. Pharm.* **2008**, *364*, 298.
- Santos-Magalhães, N. S.; Maciel, M. A. M.; Lira, M. C. B.; Morais, W. A.; Lapenda, T. L. S.; *Lat. Am. J. Pharm.* **2012**, *31*, 97.
- Klose, D.; Siepmann, F.; Elkharraz, K.; Siepmann, J.; *Int. J. Pharm.* **2008**, *354*, 95.
- Jeffery, H.; Davis, S. S.; O'Hagan, D. T.; *Pharm. Res.* **1993**, *10*, 362.
- Li, X.; Deng, X.; Yuan, M.; Xiong, C.; Huang, Z.; Zhang, Y.; Jia, W.; *Int. J. Pharm.* **1999**, *178*, 245.
- Conti, B.; Genta, I.; Modena, T.; Pavanetto, F.; *Drug Dev. Ind. Pharm.* **1995**, *21*, 615.
- Mao, S.; Xu, J.; Cai, C.; Germershaus, O.; Schaper, A.; Kissel, T.; *Int. J. Pharm.* **2007**, *334*, 137.
- Bibby, D. C.; Davies, N. M.; Tucker I. G.; *Int. J. Pharm.* **2000**, *197*, 1.
- Dong, C.-M.; Guo, Y.-Z.; Qiu, K.-Y.; Gu, Z.-W.; Feng, X.-D.; *J. Controlled Release* **2005**, *107*, 53.
- Jyothi, N. V.; Prasanna, N. P. M.; Sakarkar, S. N.; Prabha, K. S.; Ramaiah, P. S.; Srawan, G. Y.; *J. Microencapsulation* **2010**, *27*, 187.
- Makadia, H. K.; Siegel S. J.; *Polymers* **2011**, *1*, 1377.
- Ungaro, F.; De Rosa, G.; Miro, A.; Quaglia, F.; La Rotonda, M. I.; *Eur. J. Pharm. Sci.* **2006**, *28*, 423.

Submitted: August 16, 2016

Published online: January 18, 2017